
Supplementary Material:

A trait-based framework for explaining non-additive effects of multiple stressors on plankton communities

1 MODEL DESCRIPTION

Phytoplankton specific production rate (μ_i) for group “ i ” in the model is a function of light intensity, temperature, internal nutrient quotas and CO_2 (Table S2, Eq.1). All metabolic rates and remineralization rate of detritus increase with rising temperature following the Q_{10} equation or Van’t Hoff rule, resp., (f_T) (Table S3, Eq.1) (Montagnes et al., 2003). Nitrogen and phosphorous are in the model regarded as limiting nutrients of primary production and the growth rate dependency on their intracellular stores is defined by the Droop function ($q_{N,i}$ and $q_{P,i}$) (Table S1, Eq.3-4). Co-limitation by the two nutrients quotas is described by a normalized multiplicative type function (Table S1, Eq.2) (Wirtz and Kerimoglu, 2016). Light limitation ($f_{\text{PAR},i}$) follows a cumulative one-hit Poisson distribution including photoinhibition (Platt et al., 1980). This light response function also depends on cell size, temperature, and CO_2 (Table S1, Eq.5). The average light intensity ($\overline{\text{PAR}}$) over the mixed layer is obtained by the Lambert-Beer law (Table S1, Eq.18) resolving the attenuation of light due to background particles and phytoplankton biomass (Table S1, Eq.17) (Huisman and Weissing, 1995). Furthermore, the rate limitation by sub-optimal carboxylation ($f_{\text{CO}_2,i}$) is specified by a biophysically explicit description for carbon uptake as a function of cell size adopted from (Wirtz, 2011) and simplified by Moreno de Castro et al. (2017) (Table S3, Eq.6).

Table S1. Model equations. Auxiliary variables and parameters are described in Table S2– S4. The subscript i distinguishes phytoplankton size classes and j the three zooplankton classes.

| State variable | Dynamical equation | Unit |
|---|--|---------------------------|
| 1. Phytoplankton biomass | $\frac{d\text{Phy}_i}{dt} = (\mu_i - \text{Agg} - R_i - S_i)\text{Phy}_i - G_i + (\epsilon_m G_{m,i} - \sum_{k=i}^{i_{max}^m} G_{m,k})\text{Phy}_i$ | mmol-C m ⁻³ |
| 2. Cell nitrogen quota | $\frac{dQ_i^N}{dt} = V_i^N - (\mu_i - R_i)Q_i^N$ | mol-N mol-C ⁻¹ |
| 3. Cell phosphorous quota | $\frac{dQ_i^P}{dt} = V_i^P - (\mu_i - R_i)Q_i^P$ | mol-P mol-C ⁻¹ |
| 4. Ciliates biomasses ($Z_{j=1,2}$) | $\frac{dZ_{j=1,2}}{dt} = y \sum_{i=1}^n \text{Graz}_{ij} D_j^{\text{reg}} Z_j - \text{Graz}_{j3} D_3^{\text{reg}} Z_j - (m_j + \epsilon_m) Z_j^2$ | mmol-C m ⁻³ |
| 5. Copepod biomass ($Z_{j=3}$) | $\frac{dZ_{j=3}}{dt} = y \sum_{i=1}^n \text{Graz}_{ij} D_j^{\text{reg}} Z_j - (m_j + \epsilon_m) Z_j^2$ | mmol-C m ⁻³ |
| 6. N-content of detritus (Det_N) | $\frac{d\text{Det}_N}{dt} = \sum_{i=1}^n (\text{Agg} \cdot \text{Phy}_i Q_i^N) - (\phi f_T + \frac{\nu_d}{\text{MLD}}) \text{Det}_N + (1 - y) \sum_{i=1}^n G_i Q_i^N + (1 - \epsilon_m) \sum_{i=1}^n G_{m,i} Q_i^N + \sum_{j=1}^3 m_j Z_j^2 Q_j^{Z,N} \dagger$ | mmol-N m ⁻³ |
| 7. P-content of detritus (Det_P) | $\frac{d\text{Det}_P}{dt} = \sum_{i=1}^n (\text{Agg} \cdot \text{Phy}_i Q_i^P) - (\phi f_T + \frac{\nu_d}{\text{MLD}}) \text{Det}_P + (1 - y) \sum_{i=1}^n G_i Q_i^P + (1 - \epsilon_m) \sum_{i=1}^n G_{m,i} Q_i^P + \sum_{j=1}^3 m_j Z_j^2 Q_j^{Z,P} \dagger$ | mmol-P m ⁻³ |
| 8. Nitrogen conc. (N) | $\frac{dN}{dt} = \phi f_T \text{Det}_N - \sum_{i=1}^n (V_i^N \cdot \text{Phy}_i)$ | mmol-N m ⁻³ |
| 9. Phosphorous conc. (P) | $\frac{dP}{dt} = \phi f_T \text{Det}_P - \sum_{i=1}^n (V_i^P \cdot \text{Phy}_i)$ | mmol-P m ⁻³ |

†These terms are replaced with $(1 - y) \sum_{j=1}^2 \text{Graz}_{j3} D_3^{\text{reg}} Q_j^{Z,N}$ and $(1 - y) \sum_{j=1}^2 \text{Graz}_{j3} D_3^{\text{reg}} Q_j^{Z,P}$ respectively, where zooplankton is assumed as external forcing, i.e., not dynamically resolved.

Phytoplankton biomass removal is driven by aggregation (A), size dependent respiration (R_i), sinking (S_i), grazing by strict heterotrophs (G_i) and mixotrophic grazing ($G_{m,i}$). Phytoplankton cells and/or detritus particles are assumed to form aggregates that are rapidly exported from the system (Table S2, Eq.5). The strength of aggregation is in our model controlled by a dimensionless auxiliary variable for the concentration of transparent exopolymeric particles (TEP). Concentration of TEP is here suggested to depend on the temporal derivative of the internal nitrogen quota (\dot{Q}_N) of phytoplankton according to a sigmoid function (Table S3, Eq.7). This formulation reflects the correlation between TEP formation and carbon overconsumption, the latter being accompanied with a rapid decline in nutrient quotas. The respiratory loss of each size class or species, resp., is proportional to its nutrient uptake rate (Table S2, Eq.4) (Raven, 1981; Aksnes and Egge, 1991). Sinking of individual species is described by a modified Stoke's law function adopted from Wirtz (2013), which takes into account positive buoyancy of larger cells (Table S1, Eq.6). Size dependent grazing of zooplankton on phytoplankton follows a normal distribution function centered around an optimal prey size (L^*). Furthermore, smaller phytoplankton are assumed to be grazed by mixotrophic phytoplankton with larger cell size (Table S2, Eq.8).

Table S2. Primary production related rates. Parameters are described in Table S3 – Table S4.

| Description | Rate | Unit |
|---|--|-------------------------------|
| 1. Growth rate | $\mu_i = \mu_{\max,i} \cdot f_T \cdot f_{Q,i} \cdot f_{\text{PAR},i} \cdot f_{\text{CO}_2,i}$ | d^{-1} |
| 2. N-uptake rate | $V_i^N(N, Q_i^N) = v_{\max,i}^N \cdot f_T \cdot \left(\frac{N \cdot A_i^N}{v_{\max,i}^N + N \cdot A_i^N} \right) \cdot \max \left(0, \frac{Q_{\max,i}^N - Q_i^N}{Q_{\max,i}^N - Q_{\min,i}^N} \right)$ | $\text{mol-N (mol-C d)}^{-1}$ |
| 3. P-uptake rate | $V_i^P(N, Q_i^P) = v_{\max,i}^P \cdot f_T \cdot \left(\frac{P \cdot A_i^P}{v_{\max,i}^P + P \cdot A_i^P} \right) \cdot \max \left(0, \frac{Q_{\max,i}^P - Q_i^P}{Q_{\max,i}^P - Q_{\min,i}^P} \right)$ | $\text{mol-P (mol-C d)}^{-1}$ |
| 4. Respiration rate | $R_i = R^* V_i^N(N, Q_i^N)$ | d^{-1} |
| 5. Aggregation rate | $Agg = Agg^* \text{TEP} \cdot \left(\sum_{i=1}^n \text{Phy}_i Q_i^N + \text{Det}_N \right)$ | d^{-1} |
| 6. Sinking rate | $S_i = e^{-0.5 \left(\frac{q_{N,i} \cdot q_{P,i}}{0.45^2} \right)^2} \cdot e^{(0.5 L_i)} \cdot \frac{\nu_s}{\text{MLD}}$ | d^{-1} |
| 7. Grazing rate | $G_i = \sum_{j=1}^3 \text{Graz}_{ij} \cdot Z_j \cdot D_j^{\text{reg}}$ | d^{-1} |
| 8. Grazing on ciliates | $G^{\text{Cil}} = I_{\max,3} \cdot g_3 \frac{\rho_{c3} Z_{1,2}}{F_3} Z_3 D_3^{\text{reg}}$ | d^{-1} |
| 9. Mixotrophic grazing | $G_{m_i} = \Theta(L_i) I_{\max}^m G_m^{\max} \sum_{k=i-\Delta m}^i \frac{\text{Phy}_k}{H_m + \sum_{k=i-\Delta m}^i \text{Phy}_k}$ | d^{-1} |
| 10. Switching under low nutrient conditions | $G_m^{\max} = 1 - \left(1 + e^{(-20(\mu_i - 0.02))} \right)^{-1}$ | d^{-1} |
| 11. Size limitation for mixotrophic grazing | $\Theta(L_i) = \begin{cases} 1 & \text{if } L_i < 2.8 \\ 0 & \text{else} \end{cases}$ | |

Internal nutrients pools are filled by nutrient uptake as formulated by the Monod function (Morel, 1987) and reduced because of dilution by growth (Table S1, Eq.2–3). Nutrient uptake increases with ambient nutrient concentration and is down-regulated when the intracellular pool reaches a maximum (Q_{\max}) (Table S3, Eq.2–3). Changes in ciliate biomass reflect an imbalance between growth due to grazing on small size phytoplankton and grazing by copepod and density dependent mortality (Table S1, Eq.4). Copepod biomass in the model increases due to grazing on phytoplankton and ciliates and reduces as a result of density dependent mortality (Table S1, Eq.5). Particle aggregation, mortality and sloppy feeding of zooplankton fuel the detritus pools, while organic matter is remineralized to inorganic nutrients and removed from the surface ocean by sinking (Table S1, Eq.6–7). Finally, ambient nutrient pools are reduced because of uptake by phytoplankton and replenished through remineralization of detritus (Table S1, Eq.8–9). For related functions and parameters value please see Table S3–S4.

Table S3. Model sub functions and related variable parameters.

| Description (Source) | Symbol | Function | Unit |
|---|------------------------|--|---------------------------|
| 1. Temperature dependency (Montagnes et al., 2003) | f_T | $\frac{T - T_{\text{ref}}}{10}$ | |
| 2. Co-limitation (Wirtz and Kerimoglu, 2016) | $f_{Q,i}$ | $\frac{q_{N,i} \cdot q_{P,i}}{0.5(q_{N,i} + q_{P,i})}$ | |
| 3. Internal nitrogen quota dependency (Droop, 1973) | $q_{N,i}$ | $\frac{Q_i^N - Q_{\min,i}^N}{Q_i^N}$ | |
| 4. Internal phosphorous quota dependency (Droop, 1973) | $q_{P,i}$ | $\frac{Q_i^P - Q_{\min,i}^P}{Q_i^P}$ | |
| 5. Specific light limitation (Platt et al., 1980) | $f_{\text{PAR},i}$ | $\left(1 - e^{-\frac{\alpha_{\text{PAR}} \overline{\text{PAR}}}{\mu_{\max,i} \cdot f_{\text{CO}_2,i} \cdot f_T}}\right) \cdot e^{-\frac{\beta_{\text{PAR}} \overline{\text{PAR}}}{\mu_{\max,i} \cdot f_{\text{CO}_2,i} \cdot f_T}}$ | |
| 6. CO ₂ dependency (Wirtz, 2011; Moreno de Castro et al., 2017) | $f_{\text{CO}_2,i}$ | $\frac{1 - e^{-a_{\text{CO}_2} \cdot \text{CO}_2}}{1 + a^* e^{(L_i - a_{\text{CO}_2} \cdot \text{CO}_2)}}$ | |
| 7. Transparent Exopolymer Particles | TEP | $\text{TEP}_{\min} \frac{1 - \text{TEP}_{\min}}{1 + e^{(B^* Q_N + B_{\text{offs}}^*)}}$ | mmol-C m ⁻³ |
| 8. Functional response (Wirtz, 2013) | g_j | $1 - e^{-x_j}$ | |
| 9. Food processing ratio (Wirtz, 2013) | x_j | $\frac{A_{\text{zoo}} \cdot F_j}{I_{\max,j}}$ | |
| 10. Potential grazing rate of grazer Z_j on prey Phy_i (Wirtz, 2013) | Graz_{ij} | $I_{\max,j} \cdot g_j \cdot \frac{\rho_{ij} \cdot \text{Phy}_i}{F_j}$ | d ⁻¹ |
| 11. Down regulation (Wirtz, 2013) | D_j^{reg} | $\left(1 + e^{-\frac{\sum_{i=1}^n \text{Graz}_{ij} - G_{\min}}{0.05}}\right)^{-1}$ | |
| 12. Optimal ingestion rate (Wirtz, 2013) | $I_{\max,j}^*$ | $I_{\max}^{\circ} f_T \cdot e^{(\alpha + (2-\alpha)L_j^* + (\alpha-3)L_j)}$ | d ⁻¹ |
| 13. Maximum ingestion rate (Wirtz, 2013) | $I_{\max,j}$ | $I_{\max,j}^* \cdot e^{-s_j(L_j^* - \langle L' \rangle_j)^2}$ | d ⁻¹ |
| 14. Effective food concentration (Wirtz, 2013) | F_j | $\begin{cases} F_{j=1,2} = \sum_{i=1}^n \text{Phy}_i \cdot \rho_{ij} \\ F_{j=3} = \sum_{i=1}^n \text{Phy}_i \cdot \rho_{i3} + \sum_{j=1}^2 Z_j \cdot \rho_{j3} \end{cases}$ | mmol-C m ⁻³ |
| 15. Average food size (Wirtz, 2013) | $\langle L' \rangle_j$ | $\begin{cases} \langle L' \rangle_{j=1,2} = \sum_{j=1}^2 \text{Phy}_i \cdot \rho_{ij} \cdot L_i / F_{j=1,2} \\ \langle L' \rangle_{j=3} = (\text{Phy}_i \cdot \rho_{i3} \cdot L_i + \sum_{j=1}^2 Z_j \cdot \rho_{j3} \cdot L_j) / F_{j=3} \end{cases}$ | log _e ESD (μm) |

Table S4. Model sub functions and related variable parameters (continue).

| Description (Source) | Symbol | Function | Unit |
|---|---------------------|---|--------------------------------------|
| 16. Variable MLD | $MLD(t)$ | $\frac{0.4 + 0.6}{(1 + e^{(0.2(t-t_{\text{delay}})))})}$ | m |
| 17. Background turbidity (Huisman and Weissing, 1995) | k | $\epsilon \cdot (\sum_{i=1}^n \text{Phy}_i Q_i) + \kappa$ | d^{-1} |
| 18. Average light intensity within MLD (Huisman and Weissing, 1995) | \overline{PAR} | $\frac{PAR_0}{MLD} \int_0^{MLD} e^{-k \cdot z'} dz' = \frac{PAR_0}{k \cdot MLD} (1 - e^{-k \cdot MLD})$ | $\mu\text{mol m}^{-2} \text{s}^{-1}$ |
| 19. Total phytoplankton biomass | Phy_T | $\sum_{i=1}^n \text{Phy}_i$ | |
| 20. Community mean cell size | $\langle L \rangle$ | $20. \frac{1}{\text{Phy}_T} \sum_{i=1}^n L_i \cdot \text{Phy}_i$ | $\log_e \text{ESD} (\mu\text{m})$ |
| 21. Community size diversity | δL | $\frac{1}{\text{Phy}_T} \sum_{i=1}^n (L_i - \langle L \rangle)^2 \cdot \text{Phy}_i$ | $\log_e \text{ESD} (\mu\text{m})$ |
| 22. Variable Copepod body size | $L_{j=3}$ | $\frac{0.6 + 0.4}{(1 + e^{(0.2(t-t_{\text{delay}})))})}$ | $\log_e \text{ESD} (\mu\text{m})$ |
| 24. Chlorophyll a | Chl_a | $\Theta_N \sum_{i=1}^n \text{Phy}_i Q_i^N + \Theta_C \sum_{i=1}^n \text{Phy}_i$ | mg-C m^{-3} |

1.1 Model parameters

Table S5. Parameters used in the reference run

| Symbol | Value | Unit | Description |
|---------------------------|---|---|--|
| L_i | | \log_e ESD μm | Phytoplankton cell size |
| Agg^* | 0.2 | d^{-1} | Maximum aggregation rate |
| B^* | 15 | $\text{mol-N (mol-C d)}^{-1}$ | TEP related coefficient |
| B_{offs}^* | 3.5 | | TEP related coefficient |
| TEP_{min} | 0.07 | | TEP related coefficient |
| R^* | 3 | mol-C mol-N^{-1} | Respiratory C cost of N assimilation for phytoplankton |
| ν_s | 0.05 | m d^{-1} | Settling velocity of phytoplankton |
| α_{PAR} | 0.024 | $\mu\text{mol phot}^{-1}\text{m}^2\text{d}$ | Light absorption |
| β_{PAR} | 0.002 | $\mu\text{mol phot}^{-1}\text{m}^2\text{d}$ | Coefficient for photoinhibition |
| a_{CO_2} | 0.013 | μatm^{-1} | Carbon acquisition |
| a^* | 0.02 | μm^{-1} | Carboxylation depletion |
| $L_{j=1,2}$ | 2.8,3.8 | \log_e ESD μm | Zooplankton body size |
| $L_{j=3}$ | 6.2 | \log_e ESD μm | Copepod maximum body size |
| L_j^* | 1.2,1.2,3 | \log_e ESD μm | Optimal prey size for zooplankton class j |
| I_{max}^o | 173 | d^{-1} | I_{max} at $L_j = L^* = 0$ |
| $\alpha_{\text{Im},0}$ | 0.2 | | Size scaling exponent of I_{max}^* |
| α | $\alpha_{\text{Im},0}(L_j + L_j^*)$ | | Zooplankton maximum ingestion rate related parameter |
| s_j | 2.5,2.,2.2 | \log_e ESD $(\mu\text{m})^{-2}$ | Selectivity of zooplankton j |
| ρ_{ij} | $e^{-s_j(L_j^* - L_i)^2}$ | | Preference of grazer Z_j for prey Phy_i |
| ρ_{j3} | $e^{-s_3(L_3^* - L_j)^2}$ | | Preference of grazer Z_3 for prey $Z_{j=1,2}$ |
| A_{zoo} | 0.2 | $\text{m}^3(\text{mmol-C d})^{-1}$ | Grazing affinity for algal food |
| y | 0.3 | | Zooplankton growth efficiency |
| R_{zoo} | 0.3 | mmol-C m^{-3} | Specific activity respiration of grazing |
| ϵ_m | 0.2 | | Specific C overconsumption/release |
| I_{max}^m | 0.9 | d^{-1} | Maximum ingestion rate for mixotrophic grazing |
| Δm | 3 | | Number of size classes with $L_i \leq L_k$ consumable by species k |
| $m_{j=1,2,3}$ | 0.02, 0.02, 0.005 | d^{-1} | Zooplankton mortality rate |
| G_{min} | $\frac{A_{\text{zoo}} \cdot R_{\text{zoo}}}{y}$ | d^{-1} | Min. harvesting rate at which grazing starts |

Table S6. Parameters used in the reference run

| Symbol | Value | Unit | Description |
|------------------|----------------------|-------------------------------------|--|
| T_{ref} | 10 | °C | Reference temperature |
| κ | 0.2 | d^{-1} | Background turbidity |
| ϵ | 0.05 | $\text{m}^2\text{mmol-N}^{-1}$ | Light attenuation due to phytoplankton biomass |
| ϕ | 0.003 | d^{-1} | Remineralization rate of detritus |
| ν_d | 1 | m d^{-1} | Detritus sinking velocity rate |
| Q_{10} | 2 (phy.), 2.4 (zoo.) | | Rate increase at 10 °C temperature rise |
| Q_Z^N | 0.3 | mol-N mol-C^{-1} | Zooplankton internal nitrogen quota |
| Q_Z^P | 0.03 | mol-P mol-C^{-1} | Zooplankton internal phosphorous quota |
| Θ_N | 1.1 | $\text{mol Chl}_a\text{mol-N}^{-1}$ | Chl _a to nitrogen ratio |
| Θ_C | 0.006 | $\text{mol Chl}_a\text{mol-C}^{-1}$ | Chl _a to carbon ratio |

2 ALLOMETRIC RELATIONSHIPS OF PHYSIOLOGICAL TRAITS

Table S7. Size scaling of physiological parameters for phytoplankton adapted from Edwards et al. (2012) and Marañón et al. (2013). The subscript 'i' represents each phytoplankton species, V is the phytoplankton cell volume and L the natural logarithm of Equivalent Spherical Diameter.

| Description | Parameter | Original Value | Original unit | Final value | Final unit |
|--|--------------|-------------------------|---------------------------------|-------------------|-------------------------------------|
| Min. cell N-quota | Q_{\min}^N | $10^{-9.3}V_i^{0.77}$ | pg-N cells^{-1} | $0.032e^{-0.33L}$ | mol-N mol-C^{-1} |
| Min. cell P-quota | Q_{\min}^P | $10^{-10.6}V_i^{0.79}$ | pg-P cells^{-1} | $0.002e^{-0.27L}$ | mol-P mol-C^{-1} |
| Max. cell N-quota | Q_{\max}^N | $10^{-8.5}V_i^{0.9}$ | pg-N cells^{-1} | $0.183e^{0.06L}$ | mol-N mol-C^{-1} |
| Max. cell P-quota | Q_{\max}^P | $10^{-9.5}V_i^{0.89}$ | pg-P cells^{-1} | $0.018e^{0L}$ | mol-P mol-C^{-1} |
| Max. N-uptake rate | v_{\max}^N | $10^{-8.8}V_i^{0.8}$ | $\mu\text{mol-N (cell d)}^{-1}$ | $0.619e^{-0.24L}$ | $\text{mol-N (mol-C d)}^{-1}$ |
| Max. P-uptake rate | v_{\max}^P | $10^{-9.9}V_i^{0.8}$ | $\mu\text{mol-P (cell d)}^{-1}$ | $0.062e^{-0.24L}$ | $\text{mol-P (mol-C d)}^{-1}$ |
| N affinity | A^N | $10^{-7.5}V_i^{0.78}$ | L (cell d)^{-1} | $1.983e^{-0.3L}$ | $\text{m}^3 (\text{mmol-C d})^{-1}$ |
| P affinity | A^P | $10^{-7.8}V_i^{0.78}$ | L (cell d)^{-1} | $0.994e^{-0.3L}$ | $\text{m}^3 (\text{mmol-C d})^{-1}$ |
| Cell carbon content | Q_c | $10^{-0.69}V_i^{0.88}$ | pg-C cell^{-1} | $0.116e^{2.64L}$ | mol-C cell^{-1} |
| Max. growth rate $V_{\text{cell}} < 500 \mu\text{m}^3$ | μ_{\max} | $10^{-0.17}V_i^{0.035}$ | d^{-1} | $0.658e^{0.105L}$ | d^{-1} |
| Max. growth rate $V_{\text{cell}} > 500 \mu\text{m}^3$ | | $10^{-0.03}V_i^{-0.02}$ | | $0.963e^{-0.06L}$ | |

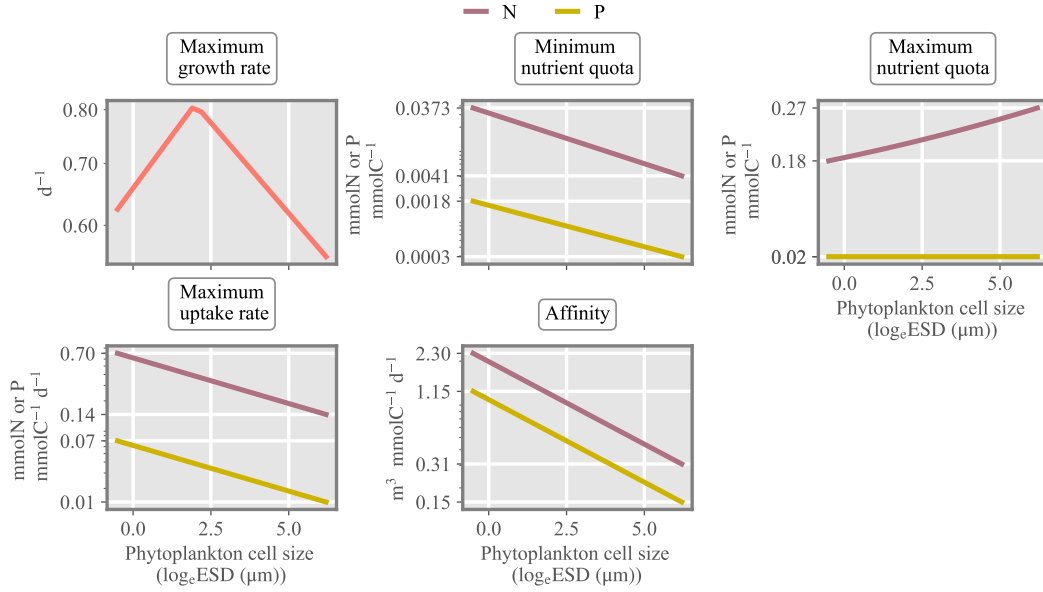


Figure S1: Allometric relationships used in the model for major growth-nutrient uptake parameters given in Table S4. Maximum growth rate is adapted from Wirtz (2011). The size range corresponds to 0.6-500 μm ESD.

3 MULTI-STRESSORS EFFECT

3.1 Specific multistressor effect size

We here introduce a generic formalism to describe stressor effects in complex systems such as phytoplankton communities or marine food-webs. The formalism specifically aims at relate (known) single stressor effects and trait dynamics to (unknown) multi-stressor effects. For doing so, we pinpoint possible determinants of the non-linear interaction between stressor reactions with special focus on internal re-organization of biological agents, here termed trait dynamics, and the trade-offs ruling that dynamics.

Consider a sudden shift in the external variable or stressor, resp., E_n , which triggers a shift in the target variable μ (e.g. growth rate, or biomass) from the unperturbed value μ^0 ($\Delta\mu = \mu - \mu^0$):

$$\Delta_n\mu = \frac{\delta\mu}{\delta E_n} \Delta E_n \quad (\text{S1})$$

where the differential $\frac{\delta\mu}{\delta E_n}$ formally expresses how sensitive μ reacts to external changes in E_n . This differential can be understood as the total derivative that also includes indirect effects not explicitly given in the growth dependencies. The concept of total derivatives in biological modeling has been proposed by (Wirtz, 2013; Wirtz and Kerimoglu, 2016).

In case of two simultaneous stressors $\Delta E_n, \Delta E_m$, we write the linear (Taylor) expansion of the total effect:

$$\Delta_{nm}\mu = \frac{\delta\mu}{\delta E_n}\Delta E_n + \frac{\delta\mu}{\delta E_m}\Delta E_m + \frac{\delta^2\mu}{\delta E_n\delta E_m}\Delta E_n\Delta E_m \quad (\text{S2})$$

While the first terms can be related to single stressor effects which may be known from lab experiments, the last term describing the combined sensitivity to both stressors n and m is in general given neither from theory nor experiments. This sensitivity is here termed the specific multi-stressor sensitivity (SMS) :

$$\text{SMS} = \frac{\delta^2\mu}{\delta E_n\delta E_m} \quad (\text{S3})$$

Under the (rough) approximation that the observed single stressor shifts $\Delta_n\mu$ and ΔE_n are similar to the respective contributions in the multi-stressor case,

$$\frac{\delta\mu}{\delta E_n} = \frac{\Delta_n\mu}{\Delta E_n} \quad (\text{S4})$$

we obtain an expression for the specific multi-stressor sensitivity depending on (observed/known) single-stressor responses $\Delta_n\mu$ and $\Delta_m\mu$ after inserting Eq.S1 into Eq. S2 and isolating the SMS:

$$\text{SMS} = \frac{\Delta_{nm}\mu - \Delta_n\mu - \Delta_m\mu}{\Delta E_n\Delta E_m} \quad (\text{S5})$$

SMS is zero for additive effects, positive for synergistic and negative for antagonistic effects.

3.2 Effective interaction traits

The interaction trait x_n with respect to stressor E_n is defined as the sensitivity of the growth rate wrt E_n

$$x_n = \frac{\partial\mu}{\partial E_n} \quad (\text{S6})$$

Note the similarity of the trait definition Eq. S6 to the effect relation Eq. S1. The first equation *formally* describes how the target variable (here growth rate μ) depends on marginal changes in an ambient factor, while the second quantifies the (again marginal) *realized* effect of μ when shifting that factor. Their respective value must not necessarily coincide because system effects such as compensation, synergies, adaptation will lead to a divergence between the formal dependency as given by the partial derivative $\frac{\partial\mu}{\partial E_n}$ and the phenomenological dependency, here written as total derivative using the perturbation notation $\frac{\delta\mu}{\delta E_n}$.

Eq. S6 in particular offers a simple and reasonable way of how to define effective trait variables. For example, if E_n denotes the grazer pressure, which in turn relates with predator concentration ($E_n = Z$), such that the phytoplankton growth rate includes a mortality term proportional to this concentration ($-g'Z$), x_Z is the negative proportionality factor, thus grazing rate per unit grazer ($-g'$). The factor is in general

formulated as the product of edibility and relative ingestion rate, and is here termed the susceptibility to grazing.

In the second case considered in our study, E_m denotes the nutrient concentration ($E_m = N$); however, due to the indirect dependency of growth on N , the formalism gets more complicated. While uptake rate V is an explicit function of the ambient nutrient concentration ($V(N)$), here formulated using the affinity A ,

$$V = v_{\max}^N \cdot \left(\frac{N \cdot A^N}{v_{\max}^N + N \cdot A^N} \right) \quad (S7)$$

the (carbon based) growth rate depends on the internal and not external nutrient availability apart of the respiration term ($-\zeta V(N)$). Following the rationale outlined by Wirtz (2013); Wirtz and Kerimoglu (2016), the marginal dependency can be derived by referring to the balance equation (Table S1-Eq2), such that we have

$$x_{N,i} \approx \frac{\partial \mu_i}{\partial Q} \frac{dQ_i}{dN} = \frac{\delta \mu_i}{\delta Q} \left[\frac{\partial V_i}{\partial N} - Q_i \frac{\partial \mu}{\partial N} \right] \cdot \left[Q_i \frac{\partial \mu_i}{Q} + \mu \right]^{-1} \quad (S8)$$

The nutrient usage ability, $x_{N,i}(\text{m}^3 (\text{mmol-C d})^{-1})$ or its averaged trait form $x_N = C_T^{-1} \sum_i x_{N,i} C_i$, with biomass C_i and total community mass C_T , incorporates three types of determinants of how a species or a community can cope with nutrient limitation: (1) The external dependency on nutrient availability that stems from the derivative term

$$\frac{\partial V_i}{\partial N} = V_i^2 (A_i N)^{-2} \cdot A_i \quad (S9)$$

predicts a diminishing x_N at high nutrient concentration, because of saturation of nutrient uptake. (2) The quota dependency of carbon based growth, $\frac{\partial \mu_i}{\partial Q}$, similarly saturates at high internal stores. This physiological determinant reflects a temporal delay in the nutrient limitation as internal stores may be decoupled from ambient nutrient level at the scale of hours to weeks. (3) At low nutrient availability with $V_i \approx A_i N$, then x_N becomes proportional to the nutrient affinity, which is a classical trait describing nutrient uptake ability.

3.3 Cross-over trait sensitivity and trade-offs

A major assumption underlying our approach is that the phenomenological dependency $\frac{\delta \mu}{\delta E_n}$ can be approximated at first order by the formal stressor dependency $\frac{\partial \mu}{\partial E_n}$, i.e.

$$\frac{\delta \mu}{\delta E_n} \approx \frac{\partial \mu}{\partial E_n} = x_n \quad (S10)$$

This relation entirely focusses on the trait mediated response and neglects system feed-backs. However, the approximation allows for a derivation of the specific multi-stressor sensitivity in terms of interrelated

changes in trait, which in turn reflect morphological or physiological trade-offs. The SMS follows from combining Eq. S3 and Eq. S10 by applying another perturbation ΔE_m and repeat the procedure with a different sequence of stressors, thus perturbing x_m w.r.t. to stressor E_n .

$$\text{SMS} \approx \frac{\delta x_n}{\delta E_m} + \frac{\delta x_m}{\delta E_n} \quad (\text{S11})$$

This procedure implies that the difference is taken from an already perturbed state instead from the ground value as in the previous formalism. The procedure and its outcome is here denoted as the cross-trait variation (CTV):

$$\text{CTV} = \frac{x_{nm} - x_m}{\Delta E_m} + \frac{x_{mn} - x_n}{\Delta E_n} \quad (\text{S12})$$

The cross-over terms describe how the effective interaction traits are modified by other stressors such as the possible alteration in susceptibility to grazing due to nutrient stress and the alteration in nutrient usage ability due to grazing. Inherent to these changes are trade-offs, thus relations between different traits. For phytoplankton communities, susceptibility to grazing x_Z is linked to nutrient usage ability x_N since both traits depend on the size structure of the community. Therefore, adaptation in x_N will induce a change in x_Z too. This change will increase with the strength of the trade-off and is inherent to the terms $\delta x_Z / \delta N$ and $\delta x_N / \delta Z$. It is in principle possible to calculate the cross-trait variations based on the formulations underlying the size-based model.

A first major outcome of this study, in mathematical terms, is the similarity between specific multi-stressor sensitivity and cross-over sensitivity in effective traits:

$$\text{SMS} \approx \text{CTV} \quad (\text{S13})$$

According to this hypothesis, synergistic effects occur at positive cross-variations in traits, thus, when effective traits shift to higher values under application of complementary stressors (e.g., increasing nutrient usage ability under grazing removal). This re-organization within the community will in general require some time so that a second prediction of our theory is a transition from antagonistic to synergistic multi-stressor effects over time.

4 SUPPLEMENTARY FIGURES

5 MONO SPECIES SCENARIO

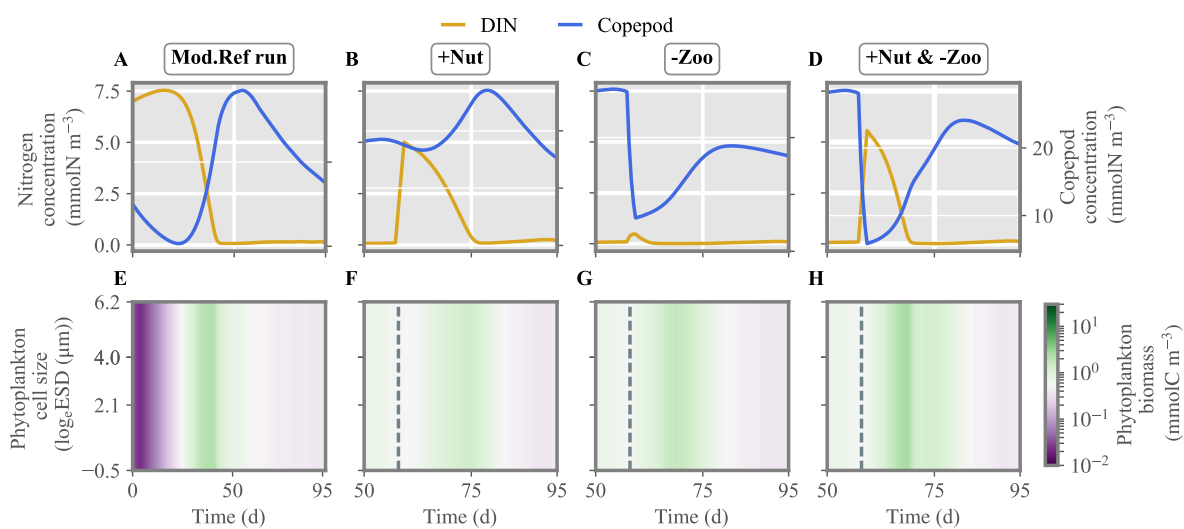


Figure S2: Mono-species model: Nitrogen concentration, copepod biomass and phytoplankton biomass distribution under single /multiple stressors. +Nut and -Zoo represent two stressors corresponding to nutrient enrichment and grazer removal. Dashed lines indicate the time of nutrient injection, zooplankton removal or both.

6 SENSITIVITY ANALYSIS

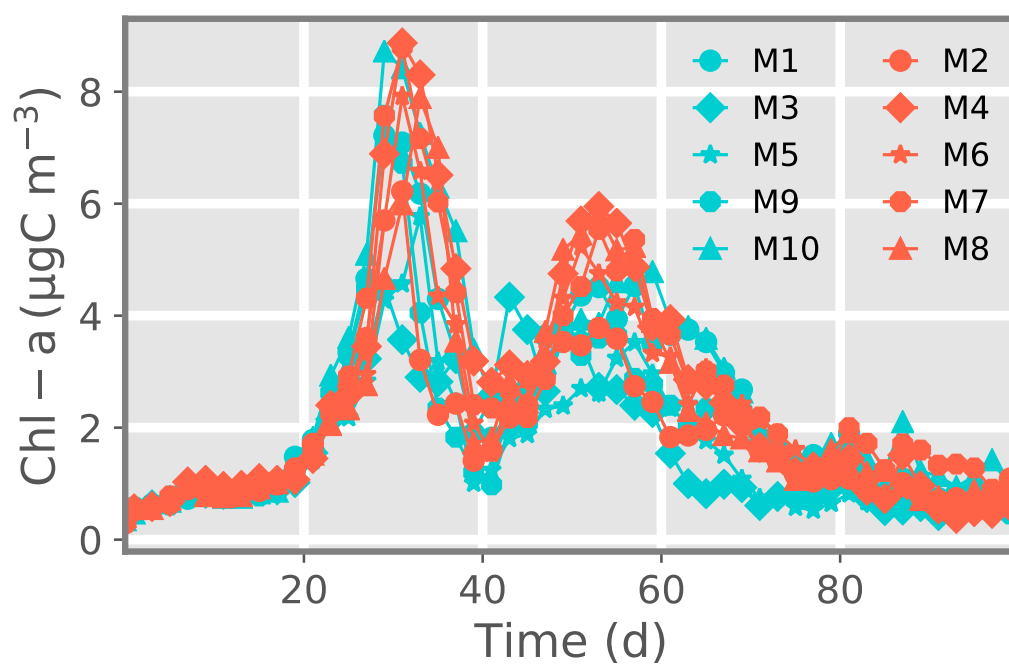


Figure S3: Measured Chl-a for 10 Kristineberg mesocosms from (Bach et al., 2016). Red and blue indicate High CO₂ and low CO₂ conditions respectively.

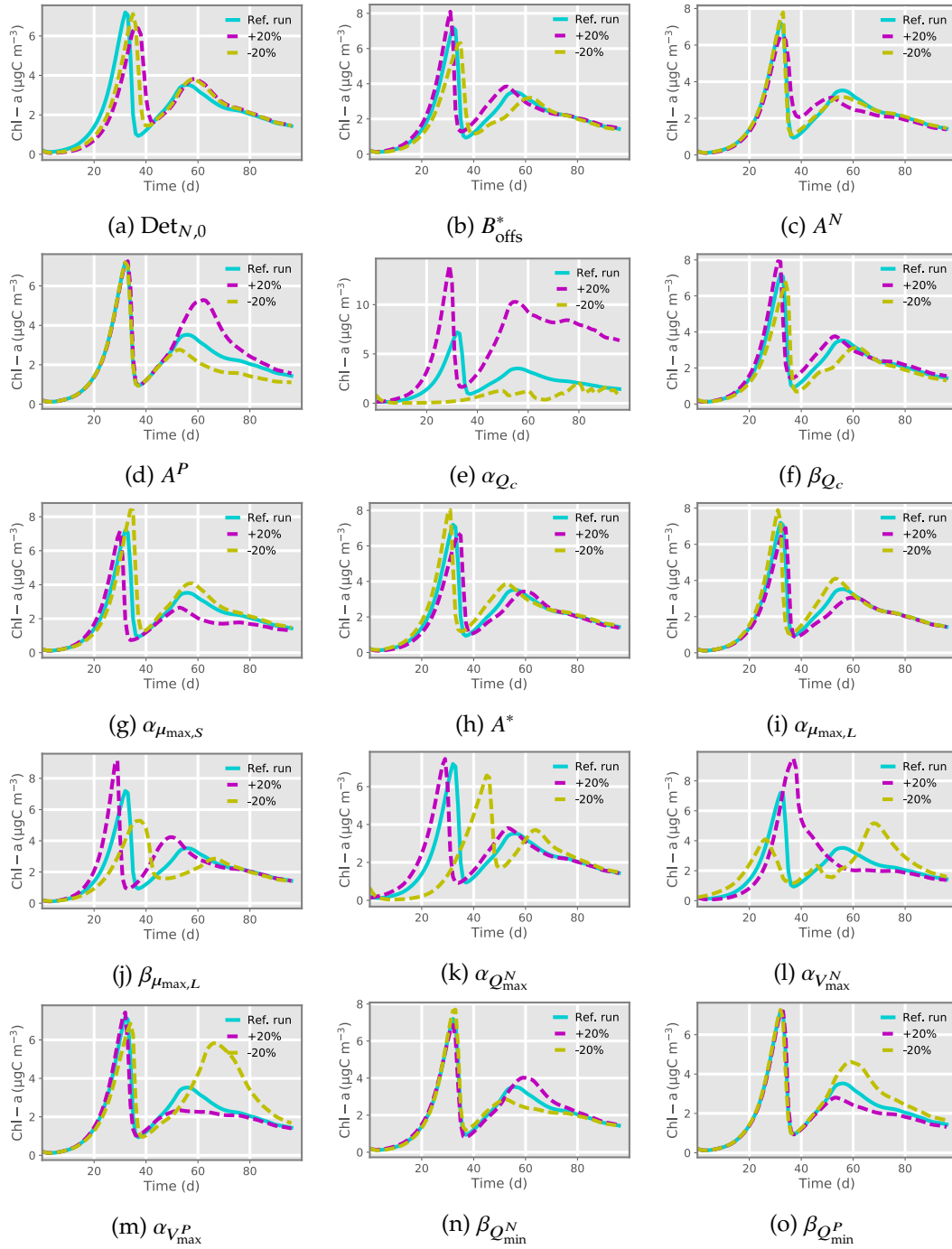


Figure S4: Sensitivity analysis for Chl simulated in the reference configuration for low pCO_2 condition. Parameters are varied by $\pm 20\%$ of their original value. Descriptions and reference values of the parameters are listed in Tables S4 and S5.

REFERENCES

Aksnes, D. L. and Egge, J. K. (1991). A theoretical model for nutrient uptake in phytoplankton. *Marine Ecology Progress Series* 70, 65–72

- Bach, L. T., Taucher, J., Boxhammer, T., Ludwig, A., Consortium, T. K. K., Achterberg, E. P., et al. (2016). Influence of ocean acidification on a natural winter-to-summer plankton succession: First insights from a long-term mesocosm study draw attention to periods of low nutrient concentrations. *PLOS ONE* 11, 1–33
- Droop, M. R. (1973). Some thoughts on nutrient limitation in algae. *Journal of Phycology* 9, 264–272
- Edwards, K. F., Thomas, M. K., Klausmeier, C. A., and Litchman, E. (2012). Allometric scaling and taxonomic variation in nutrient utilization traits and maximum growth rate of phytoplankton. *Limnology and Oceanography* 57, 554–566. doi:10.4319/lo.2012.57.2.0554
- Huisman, J. and Weissing, F. (1995). Competition for nutrients and light among phytoplankton species in a mixed water column: Theoretical studies. *Water Science and Technology* 32, 143–147
- Marañón, E., Cermeño, P., López-Sandoval, D. C., Rodríguez-Ramos, T., Sobrino, C., Huete-Ortega, M., et al. (2013). Unimodal size scaling of phytoplankton growth and the size dependence of nutrient uptake and use. *Ecology Letters* 16, 371–379
- Montagnes, D. J., Kimmance, S. A., and Atkinson, D. (2003). Using Q10: can growth rates increase linearly with temperature? *Aquatic Microbial Ecology* 32, 307–313
- Morel, F. M. M. (1987). Kinetics of nutrient uptake and growth in phytoplankton. *Journal of Phycology* 23, 137–150
- Moreno de Castro, M., Schartau, M., and Wirtz, K. (2017). Potential sources of variability in mesocosm experiments on the response of phytoplankton to ocean acidification. *Biogeosciences* 14, 1883–1901
- Platt, T., Gallegos, C. L., and Harrison, W. G. (1980). Photoinhibition of photosynthesis in natural assemblages of marine phytoplankton. *Journal of Marine Research* 38, 687–701
- Raven, J. (1981). Nutrient transport in microalgae. *Advances in Microbial Physiology* 21, 47 – 226
- Wirtz, K. W. (2011). Non-uniform scaling in phytoplankton growth rate due to intracellular light and CO₂ decline. *Journal of Plankton Research* 33, 1325–1341. doi:10.1093/plankt/fbr021
- Wirtz, K. W. (2013). Mechanistic origins of variability in phytoplankton dynamics: Part I: niche formation revealed by a size-based model. *Marine Biology* 160, 2319–2335
- Wirtz, K. W. and Kerimoglu, O. (2016). Autotrophic stoichiometry emerging from optimality and variable co-limitation. *Frontiers in Ecology and Evolution* 4, 131